Effective viscosity in quantum turbulence: a steady-state approach

Simone Babuin, Emil Varga, Ladislav Skrbek, Emmanuel Lévêque, Philippe-Emmanuel P.-E. Roche

▶ **To cite this version:**

Simone Babuin, Emil Varga, Ladislav Skrbek, Emmanuel Lévêque, Philippe-Emmanuel P.-E. Roche. Effective viscosity in quantum turbulence: a steady-state approach. EPL - Europhysics Letters, 2014, 106 (2), pp.24006. 10.1209/0295-5075/106/24006 . hal-00984313v2

HAL Id: hal-00984313
https://hal.science/hal-00984313v2

Submitted on 24 Feb 2015

HAL is a multi-disciplinary open access archive for the deposit and dissemination of scientific research documents, whether they are published or not. The documents may come from teaching and research institutions in France or abroad, or from public or private research centers.

L'archive ouverte pluridisciplinaire **HAL**, est destinée au dépôt et à la diffusion de documents scientifiques de niveau recherche, publiés ou non, émanant des établissements d'enseignement et de recherche français ou étrangers, des laboratoires publics ou privés.

Effective viscosity in quantum turbulence: a steady-state approach

Simone Babuin[1], Emil Varga[2], Ladislav Skrbek[2], Emmanuel Lévêque[3,4] and Philippe-E. Roche[5,6]

[1] *Institute of Physics ASCR, Na Slovance 2, 182 21 Prague, Czech Republic*
[2] *Faculty of Mathematics and Physics, Charles University in Prague, Ke Karlovu 3, 121 16 Prague, Czech Republic*
[3] *Laboratoire de Physique, Ecole Normale Supérieure de Lyon & CNRS, Université de Lyon, 46 allée d'Italie, F-69364 Lyon cedex 7, France*
[4] *Laboratoire de Mécanique des Fluides et d'Acoustique, Ecole Centrale de Lyon & CNRS, Université de Lyon, 36 avenue Guy de Collonge F-69134, Ecully, France*
[5] *Univ. Grenoble Alpes, Inst NEEL, F-38042 Grenoble, France, EU*
[6] *CNRS, Inst NEEL, F-38042 Grenoble, France, EU*

PACS 47.37.+q – Hydrodynamic aspects of superfluidity; quantum fluids
PACS 67.57.De – Superflow and hydrodynamics
PACS 67.40.Vs – Vortices and turbulence

Abstract. - The concept of "effective viscosity" ν_{eff} of superfluid helium, widely used to interpret decaying turbulence, is tested in the steady-state case. We deduce ν_{eff} from measurements of vortex line density, $\mathcal{L}$, in a grid flow. The scaling of $\mathcal{L}$ with velocity confirms the validity of the heuristic relation defining ν_{eff}, $\epsilon = \nu_{\text{eff}} (\kappa\mathcal{L})^2$, where ϵ is the energy dissipation rate and κ the circulation quantum. Within $1.17 - 2.16\,\text{K}$, ν_{eff} is consistent with that from decays, allowing for uncertainties in flow parameters. Numerical simulations of the two-fluid equations yield a second estimation of ν_{eff} within an order of magnitude with all experiments. Its temperature dependence, more pronounced in numerics than experiments, shows a cross-over from a viscous-dominated to a mutual-friction-based dissipation as temperature decreases, supporting the idea that the effective viscosity of a quantum turbulent flow is an indicator of the dissipative mechanisms at play.

Introduction. – Quantum turbulence (QT) is the turbulent state of a superfluid [1–3], a fluid with quantum mechanical effects at macroscopic scale. Here we focus on He-II, the superfluid phase of liquid ^{4}He occurring below a transition temperature $T_\lambda \approx 2.18$ K. According to Landau and Tisza's two-fluid-model, He-II can be viewed as a mixture of a normal component which is viscous and entropic and a superfluid component which is inviscid and entropy-free. When He-II is stirred, the normal component supports a vorticity field as in a classical fluid while the situation for the superfluid is unique. Since the superfluid velocity is proportional to the phase gradient of a macroscopic wave function, all its vorticity is concentrated along Å-thick vortex filaments with quantized velocity circulation. The classical limit of macroscopic superfluid rotation can be recovered thanks to the partial polarisation of large number of such quantized vortices. Their presence allows exchange of momentum between the normal and superfluid components. In co-flow turbulent He-II (when both components are forced simultaneously by mechanical means), this coupling is so efficient that both superfluid and normal fluid are locked at large scales of the flow [1,2], but what happens at intermediate and microscopic scales is an active field of research.

Over the last decades, the experimental exploration of ^{4}He QT followed two independent approaches, based either on steady-state or on temporal decay. In the steady-state approach, measured quantities are often compared to their well-established counterparts in classical turbulence: examples are the pressure drop along pipes [4] and velocity spectra [5]. In the decay approach, a model has been widely used to analyse measurements and determine an "effective (kinematic) viscosity" ν_{eff} of He-II from $\simeq 100\,\text{mK}$ up to nearly T_λ [6–9][1]. To the best of our knowledge this concept of "effective viscosity" has never

[1] For an alternative model of decay, see [3, 10]

been transposed to steady-state QT. The motivation of this work is to revisit and test this concept for such flows, by experimental and numerical means.

It is useful to recall here the definition of $\nu_{\rm eff}$. To interpret the time dependence of the mean vortex line density $\mathcal{L}(t) \sim t^{-3/2}$ observed in decaying QT experiments [11], a proportionality relation has been assumed between $\mathcal{L}^2$ and the decay rate $\epsilon \equiv -dE/dt$ of the kinetic energy per unit mass [11–14]:

$$\epsilon = \nu_{\rm eff} \left(\kappa \mathcal{L}\right)^2 , \tag{1}$$

where $\kappa \simeq 10^{-7}$ m^2/s is the quantum of circulation of superfluid ^{4}He. Eq. (1) lacks a rigorous theoretical justification and was motivated by analogy with the classical turbulence equation, $\epsilon = \nu \langle \omega^2 \rangle$, linking dissipation with viscosity, ν, and vorticity, ω. When complemented with additional hypothesis discussed later, Eq. (1) has proven operational reliability in various flows undergoing turbulence decay [9]. Continuing this analogy with classical turbulence, it is interesting to recast Eq. (1) by defining the superfluid Reynolds number:

$$Re_\kappa \equiv \frac{\epsilon^{1/3} H^{4/3}}{\kappa} \equiv \frac{vH}{\kappa} , \tag{2}$$

where v and H are characteristic velocity and length scales of the flow: v is defined as the root mean square (rms) of velocity fluctuations[2], and H, representing the typical large scale of the flow, is defined as

$$H \equiv v^3/\epsilon. \tag{3}$$

In classical homogeneous isotropic turbulence, $H \simeq 2L_{11} \simeq 4L_{22}$, where L_{11} and L_{22} are the longitudinal and transverse integral scales of the flow defined from the autocorrelation function of longitudinal or transverse velocity fluctuations [15]. Introducing the mean inter-vortex spacing $\delta \equiv \mathcal{L}^{-1/2}$, Eq. (1) becomes:

$$\frac{\delta}{H} = \left(\frac{\nu_{\rm eff}}{\kappa}\right)^{1/4} Re_\kappa^{-3/4} . \tag{4}$$

This equation is equivalent to the heuristic relation (1), but turns out to be more convenient to analyze steady-state QT. As pointed out in Ref. [16], Eq. (4) is reminiscent of the equation in classical turbulence relating the Kolmogorov's viscous scale η to the integral scale: $\eta/H \simeq Re^{-3/4}$, where Re is defined as Re_κ after substitution of the kinematic viscosity for κ. Interestingly, the prefactor $\nu_{\rm eff}/\kappa$ can be seen as the effective "Schmidt number" of He-II, accounting for the ratio of a viscous dissipative process and vortex diffusivity process.

We next present a systematic experimental test of Eq. (1) over 8 orders of magnitude. The explored temperature range $1.17\,{\rm K} \leq T \leq 2.16\,{\rm K}$ generalizes the only previous experimental determination restricted around 1.55 K [16]. We then present and discuss our numerical simulations over the same temperature range.

[2]In co-flow He-II QT, as in classical turbulence, most kinetic energy resides at large scales where both components are locked, thus v is defined as the common velocity fluctuation of the two components, $v = v_n = v_s$ along an arbitrary direction.

The experiment. – The steady-flow is a mechanically forced turbulent He-II co-flow through a square cross-section channel, illustrated with dimensions in the insert of Fig. 1. It is installed vertically next to a stainless steel bellows (shown in Ref. [17]) in a liquid ^{4}He bath. The bellows is operated by a computer-controlled motor and can produce flow velocities constant to within 3%. According to the thermometers in the bath and inside the bellows, the helium temperature is maintained constant to within 0.1 mK. The lower entry of the channel has a flow conditioner made by 10 mm long capillaries of 1 mm diameter, cutting larger scale turbulent eddies. In one experiment a grid has been added to the channel, with square openings 0.5 mm wide and tine size 0.1 mm.

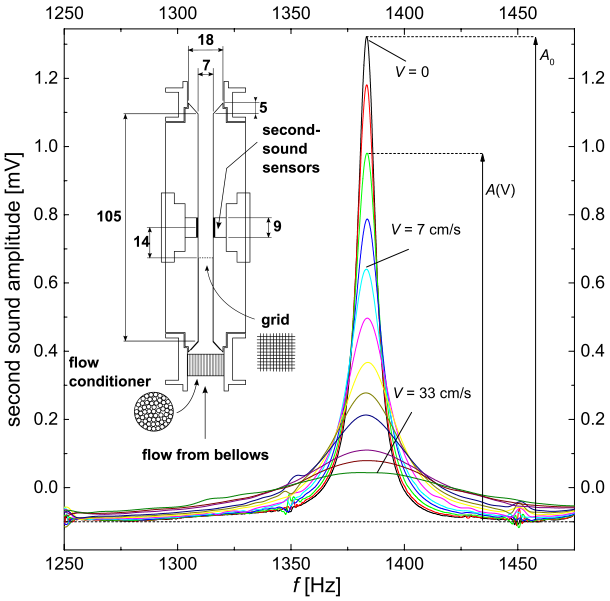

Fig. 1: Second-sound resonances for flows of different mean velocities, past the grid, at $T = 1.65$ K. The amplitude reduction relative to the $V = 0$ case enters the calculation of the vortex line density, $\mathcal{L}$. Inset: flow channel (units are mm). The flow is driven at constant velocity by a bellows.

QT is detected by the second-sound attenuation technique [17]. Quantized vortex lines scatter thermal excitations composing the normal component of He-II, thereby attenuating second-sound – here its standing wave resonance perpendicular to the mean flow direction is modified compared to quiescent helium (see Fig. 1), allowing to deduce the density of quantized vortex lines, $\mathcal{L}$. Assuming a homogeneous and isotropic tangle with $\mathcal{L} \lesssim 10^7$ cm^{-2}, then $\mathcal{L}$ can be estimated as [17]

$$\mathcal{L}(V) = \frac{6\pi \Delta f_0}{B\kappa} \left(\frac{A_0}{A(V)} - 1\right), \tag{5}$$

where Δf_0 and A_0 are the width and the amplitude of the

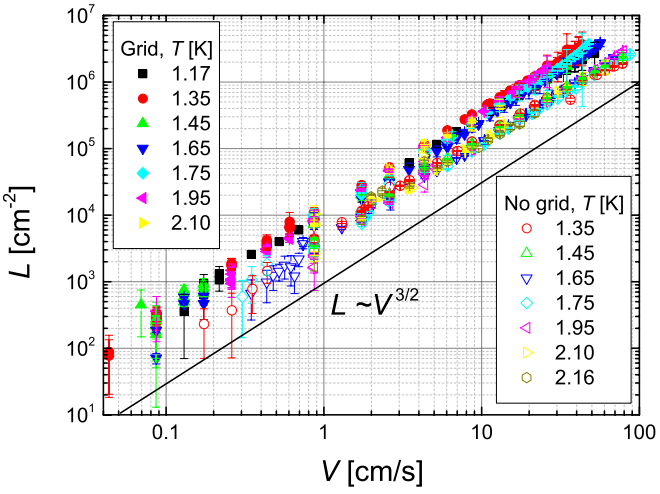

Fig. 2: The measured vortex line density as a function of mean flow velocity for the experiments with and without grid. Four decades of $\mathcal{L}$ exhibit a $V^{3/2}$ scaling, without appreciable temperature dependence, despite varying ρ_s/ρ_n from 45 to 0.1.

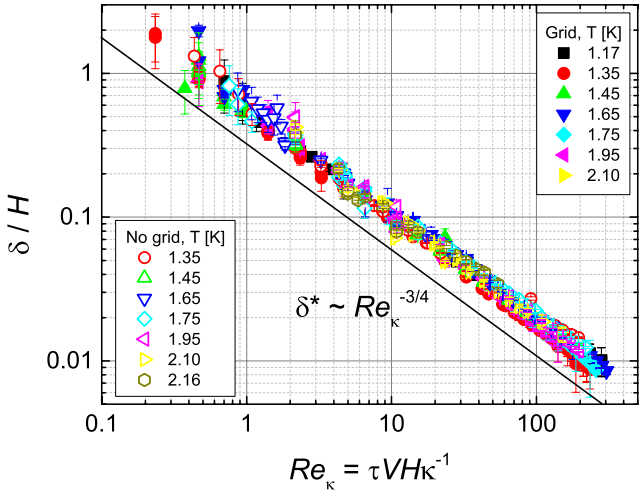

Fig. 3: Data from Fig. 2 presented as dimensionless inter-vortex spacing vs superfluid Reynolds number. The small scale of QT scales with large scale Reynolds number in analogy to viscous dissipation scale in classical turbulence. Fourteen grid and no-grid datasets collapse with an appropriate choice of the large scale of the flow, H, and turbulence intensity, τ.

resonant second-sound curve for quiescent helium, whilst $A(V)$ is the attenuated amplitude for flow velocity V; B is the mutual friction coefficient.

Experimental results. – Fig. 2 represents the primary experimental result of this paper, showing the vortex line density $\mathcal{L}$ as a function of mean flow velocity V. The data display a robust power law of the form $\mathcal{L} \propto V^{3/2}$, over about 4 orders of magnitude in $\mathcal{L}$, holding true upon changing ρ_s/ρ_n from 45 to 0.1. The presence of the grid does not change the scaling but produces about twice $\mathcal{L}$ at all velocities.

The data in Fig. 2 are replotted in Fig. 3 with coordinates δ/H versus $Re_\kappa = \tau V H/\kappa$, as suggested by Eq. (4), with $\tau = \sqrt{\langle v^2 \rangle}/V$ being the turbulence intensity. In this experiment H and τ cannot be measured directly, and are therefore treated as adjustable parameters. We make a choice of H and τ to collapse the data in Fig. 3, with the additional assumption that these parameters do not depend on Re_κ and temperature. This is generally admitted in classical turbulence (e.g. behind a grid [18] or behind a honeycomb flow conditioner [19]), and has been verified in superfluid grid turbulence down to ~ 1.6 K [5]. The fit yields H and τ consistent with typical values from classical and QT grid turbulence (see below). We stress however that we cannot independently and directly verify the independence on Re_κ and temperature, nor the exact nature of the turbulence in the probed region, which in general could be partly altered by the boundary layer of the channel [20]. In the case of flow without grid, we obtain $H = 1\,\mathrm{mm}/2 = 0.5\,\mathrm{mm}$ (1 mm is the flow conditioner capillary diameter, $2 \sim \sqrt{s_{in}/s_{out}}$ is the channel contraction estimated from cross-sections ratio [21]) and $\tau = 5\%$, a typical value for grid turbulence. In the case with grid, we obtain $H = 0.6\,\mathrm{mm}$ (mesh size) and $\tau = 9\%$, an reasonable value for turbulence in the probed region which spans from 16 to 31 mesh sizes behind the grid. At 31 meshes, $\tau \simeq 4\%$ is expected [21] while τ is expected to be more typical of jet turbulence ($\tau = 25\%$) a few mesh-sizes behind the grid[3]. With this choice of τ and H we obtain a collapse of our fourteen grid and no-grid datasets in Fig. 3 and Eq. (4) suggests that, in the explored temperature range, $\nu_{\mathrm{eff}}/\kappa$ is roughly constant.

Numerical simulations. – To estimate the effective viscosity from simulations, the numerical model should account consistently for the dominant dissipative processes in our steady turbulent flow: the viscosity of the normal component and the dissipative energy exchange between the normal and superfluid components. At present, only the so-called continuous model (where the details of individual vortices are smoothed out) has demonstrated such capacity [22]. We solve those equations in a cubic domain with periodic boundary conditions in the three directions. Accounting for this periodicity, the equations are integrated in the Fourier domain up to a truncating wavenumber $k_{\max} \equiv \pi/\delta_{\min}$, where the resolution $\delta_{\min}$ is of the order of the mean vortex line spacing δ. In order to avoid arbitrariness, the ratio $r = \delta_{\min}/\delta$ is kept as a free parameter (close to unity). The inter-vortex spacing δ is

$$\kappa.\delta^{-2} = \kappa.\mathcal{L} = \sqrt{\langle |\omega_s|^2 \rangle}, \qquad (6)$$

[3] Alternative estimations of H consistent in magnitude are from (a) the downstream growth of the classical integral length scale in grid turbulence [21]; (b) analogy with the towed grid He-II experiment [12] which yielded the time at which H is assumed to reach the channel width. In steady flow, this time translates into a ≈ 20 cm downstream distance (120 mesh units), suggesting that H is still significantly smaller than the channel width at our probe location.

where brackets denote a space average and ω_s is the (macroscopic) superfluid vorticity. Let us notice that the second equality in Eq. (6) does not account for a possible fraction of excitations along individual vortices at scales smaller than δ, which would contribute to $\mathcal{L}$ but not to ω_s. Such excitations, continuously generated by vortex reconnections, are efficiently damped above 1 K compared to random excitations larger that δ [23] and are therefore expected to represent a small correction absorbed into the free parameter r. The mutual friction force per unit volume between the superfluid and the normal fluid is approximated at first order by $\mathbf{F} = \pm\frac{B}{2}\frac{\rho_n\rho_s}{\rho}|\omega_s|\,(\mathbf{v_s} - \mathbf{v_n})$. Further details about this model, and a physical justification of its relevance above 1 K, are provided in Ref. [16].

Present simulations extend [16] by accounting for possible variations of the scale ratio r, the temperature dependence of the mutual friction parameter B and the normal fluid viscosity μ. The effective viscosity, defined by Eq. (1), is directly computed from the rate of energy injection by $\nu_{\rm eff} = \epsilon/\langle|\omega_s|^2\rangle$, without the need to compute τ and H.

A random forcing is applied at low wavenumbers on both fluid components (in proportion to their relative densities) in such a way that the total rate of energy injection ϵ remains constant over time. A pseudo-spectral method [24] is used for spatial discretization with resolution 512^3 (1024^3 at the lowest temperature). The solution is advanced in time using the second-order Adams-Bashforth scheme. Validation tests have been performed to check that $\nu_{\rm eff}$ is not significantly affected by a threefold change of Re_κ. Calculations are performed at eight temperatures between 1.19 and 2.16 K, for values of the scale ratio $r \simeq 0.6$, 1.2 and 2.4 $\pm 20\%$ (for each temperature) and within $533 \lesssim Re_\kappa \lesssim 1719$.

The calculated effective viscosities are shown in Fig. 4. At high temperature, $\nu_{\rm eff}$ approaches the kinematic viscosity μ/ρ (orange line) irrespective of r. In particular, we note a sharp increase of $\nu_{\rm eff}$ between 2 and 2.16 K. This is consistent with the expectation that at high temperature the two-fluid dynamics becomes governed by the normal component, which itself follows the classical result $\epsilon = \mu/\rho\langle|\omega_n|^2\rangle$. Indeed, the strong mutual friction between the two components then entails:

$$\nu_{\rm eff} = \frac{\epsilon}{\langle|\omega_s|^2\rangle} \simeq \frac{\epsilon}{\langle|\omega_n|^2\rangle} \simeq \mu/\rho. \qquad (7)$$

At lower temperature, $\nu_{\rm eff}$ is found to depart from the kinematic viscosity μ/ρ and some dependence with the adjustable parameter r appears. For $r \simeq 2.4$ and $T \simeq 1.19$ K, where $\rho_s/\rho_n = 40$, $\nu_{\rm eff}$ is typically one decade smaller than in the high temperature limit. To interpret this we consider that in the limiting case of a random vortex tangle moving in a quiescent normal component: it is straightforward[4] to derive the energy dissipation rate (per unit mass) from the friction of a vortex against the normal component: $\epsilon = (\rho_s\rho_n/\rho^2)(B/2)\kappa\,(\kappa\mathcal{L})^2$. This asymptotic model

[4]E.g. from Eq. (62) in [1] where $2\alpha\rho = B\rho_n$ and taking $v_L \simeq \kappa/\delta$.

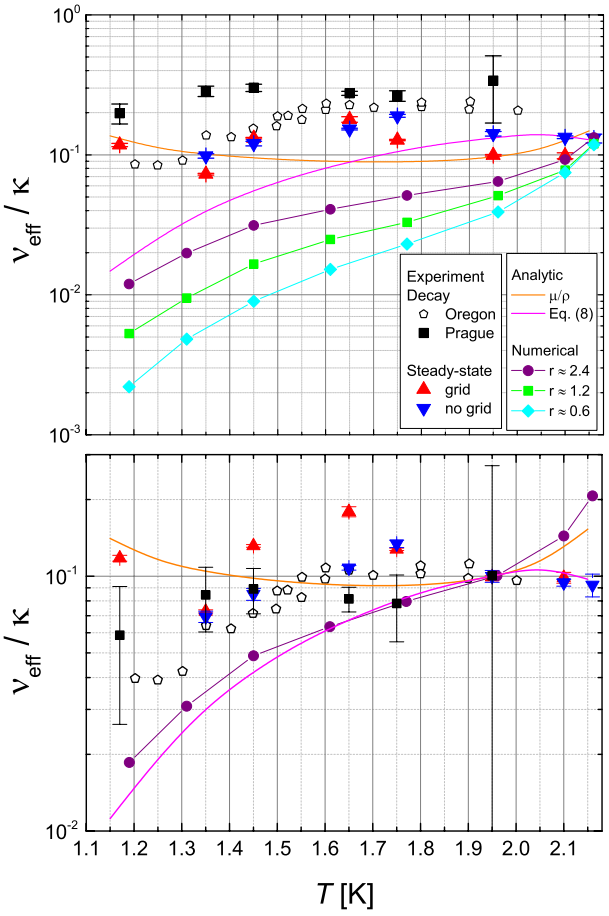

Fig. 4: (top) Dimensionless effective kinematic viscosity versus temperature. Experimental data from decay and present steady-state experiments are shown, as well as the present simulations and analytic models. The Prague decay data was measured in the same grid experiment which yielded the steady-state values of $\nu_{\rm eff}$. The numerical simulations are for three values of the scale ratio r. The solid lines represent analytic models of viscosity discussed in the text. (bottom) The data from the top panel are shown here with an offset along the y-axis so that $\nu_{\rm eff}/\kappa = 0.1$ at $T \simeq 1.96$ K for all datasets. Since the absolute value of $\nu_{\rm eff}$ is subject to uncertainties discussed in the text, this plot focusses on the temperature dependence.

of pure mutual-friction dissipation leads to:

$$\nu_{\rm eff} = \frac{\epsilon}{(\kappa\mathcal{L})^2} = \frac{\rho_s\rho_n}{\rho^2}\frac{B}{2}\kappa\,, \qquad (8)$$

shown in Fig. 4 as a solid magenta line. The temperature dependence of Eq. (8) on the low temperature side is found in good agreement with the numerical simulation data, suggesting that mutual friction, contributes significantly to dissipation below ≈ 1.5 K. The simple analytical models shows that the temperature dependence of $\nu_{\rm eff}$ found in numerical simulations can therefore be interpreted calling in a viscous dissipation process at high temperature, gradually supplemented by a mutual-friction dissipation

process at lower temperature[5].

Discussion on the validity of the heuristic equation $\epsilon = \nu_{\rm eff}\,(\kappa\mathcal{L})^2$. – As mentioned above, Eq. (1) is often assumed in order to interpret the temporal decay of $\mathcal{L}(t)$ in QT experiments, however, the interpretation also relies on additional hypothesis, the key one being that H grows in the early stages of the decay, till it saturates due to finite container size and remains constant at later times [9]. Assuming that the saturation of H is verified, it is straightforward to derive a late decay law from Eqs. (1) and (3):

$$\kappa\mathcal{L}(t) = \frac{H}{\sqrt{\nu_{\rm eff}}}\cdot t^{-3/2}. \tag{9}$$

Proportionality between $\mathcal{L}(t)$ and $t^{-3/2}$ has been reported in a number of experiments. This tends to support the validity of Eq. (1), but it cannot be considered as a direct evidence, due to the additional hypothesis on the saturation of H. For instance, another decay scenario has been proposed to interpret the $\mathcal{L}(t)$ dependence without resorting to Eq. (1), and simply assuming that the decrease of $\mathcal{L}(t)$ results from a diffusion process of the vortex tangle [3,10] (note however arguments against it in Ref. [2]).

Steady-state studies are able to provide a direct test of proportionality between ϵ and $\mathcal{L}^2$. Indeed, Eq. (4), which is equivalent to the heuristic Eq. (1), can be written in a form analogous to Eq. (9):

$$\kappa\mathcal{L} = \sqrt{\frac{\tau^3}{\nu_{\rm eff}H}}\cdot V^{3/2}. \tag{10}$$

Proportionality between $\mathcal{L}$ and $V^{3/2}$ has been reported in a narrow temperature range around 1.55 K [16]. We note also however, that a study [25] with bellows-driven He-II and second-sound pulse probe yielded $\mathcal{L}\sim V^p$, with p displaying a significant temperature dependence from 1.3 at 1.5 K to 0.9 at 2.0 K. In the present work instead, proportionality between $\mathcal{L}$ and $V^{3/2}$ is found from 1.17 up to 2.16 K in runs with and without grid (see Fig. (2)). This result can therefore be interpreted as a strong direct evidence of the validity of Eq. (1). Noteworthily, proportionality is verified down to Re_κ of order 1; this observation is consistent with the surprising ability of Eq. (9) to account for the decay of turbulence down to very low Re_κ.

On the accuracy in the determination of $\nu_{\rm eff}$. – Accuracy in determination of $\nu_{\rm eff}$ from decay and steady-state experiments is limited by uncertainties in H and τ in Eqs. (9) and (10). In decay experiments, the saturated value of H has to be estimated from the container size D i.e. the channel width, which implies some modeling of flow at large scales. This is often done using the model proposed in [12] which assumes that, in the late decay, a Kolmogorov energy spectrum $E(k) = C_k\epsilon^{2/3}k^{-5/3}$ extends up to the scale $k = 2\pi/D$ where it is truncated abruptly, which leads to Eq. (9) with $H = D(3C_k)^{3/2}/2\pi \simeq 1.5D$ (where $C_k \simeq 1.5$ is the Kolmogorov constant). This model does not account for second-order effects, such as the anisotropy resulting from the saturation on the container walls, the geometrical shape of the container, the triadic interactions around $k = 2\pi/D$, etc. If we assume uncertainty on H/D of a factor 2, the resulting uncertainty on $\nu_{\rm eff}$ is a factor 4. In the steady-state approach, both H and τ have to be estimated to determine $\nu_{\rm eff}$ from Eq. (10). In the present experiment, the uncertainty is typically a factor of 2.5 for H and a factor of 1.5 for τ, so the resulting uncertainty on $\nu_{\rm eff}$ can wind up to a factor of about 8. Moreover, both for the decay and steady-state approaches when the second-sound attenuation technique is used, $\mathcal{L}$ suffers intrinsic uncertainties of order 30% due to unknown vortex tangle distribution [17], and for our steady-state experiment an additional underestimation of $\mathcal{L}$ of order 30% is due to a denser distribution of vortex lines near the walls where the fundamental second-sound resonant mode used here is less sensitive. Cumulatively, uncertainties on L, τ and H can lead to an uncertainty on $\nu_{\rm eff}$ up to a factor of 10. These estimations illustrate the challenge of obtaining accurate experimental values of $\nu_{\rm eff}$. At any rate, a favourable constraint for the tuning of H and τ is that $\nu_{\rm eff}$ is expected to join the known value of viscosity of He-I $\nu \cong 0.167\kappa$ across the λ-point, assuming that $\kappa\mathcal{L} \to \langle|\omega_{\rm n}|^2\rangle^{1/2}$ for $T \to T_\lambda$. The accuracy could be improved by directly measuring velocity statistics at large scales for more direct inference of H and τ.

In Fig. 4 (top), $\nu_{\rm eff}/\kappa$ is obtained by fitting Eq. (10) to the data in Fig. 2 using H and τ as for Fig 3. Here error bars only reflect uncertainty on relative temperature dependence. We also show values of $\nu_{\rm eff}$ deduced from the Oregon [26] and recent Prague decay experiments [27]. The latter are significant because these are decay measurements of the flow which yielded the steady-state grid data: they are performed in the same channel, and during the same run. Given the difficulty in obtaining accurate values of $\nu_{\rm eff}$, the experiments can be considered in relatively good agreement with each other, and in the light of the almost factor 10 uncertainty, the agreement can be regarded as rough but real with the simulation too, in particular for the adjustable parameter $r \simeq 2.4$.

On the temperature dependence of $\nu_{\rm eff}$. – A comparison of the temperature dependencies is delicate because: (i) we lack experimental proof that H and τ are truly temperature independent; (ii) the experimentally observed temperature dependence of the vortex tangle polarization [28] may affect $\nu_{\rm eff}$ via Eq.(1) in ways unaccountable by the models; (iii) the pronounced frequency dependence of the mutual friction parameter $B(T)$, known to exhibit a two-fold variation from 1 Hz to 10 kHz for $1.2 < T < 2$ K [29], is ignored in the numerics and models where we chose intermediate values of B. Bearing this in mind, we shall now discuss Fig. 4 (bottom), where an arbitrary vertical offset is applied to the data in the top

[5] Below 1 K, alternative dissipation mechanisms are expected to become relevant (e.g. see review in [10]).

panel, to focus on the temperature dependence.

In the range $1.35\,K \leq T \leq 2.05\,K$ the temperature dependence from all results exhibits no significant difference within the scatter of points. For $T \gtrsim 2$ K, the sharp increase of $\nu_{\rm eff}(T)$ seen in the simulations is not found in experiments. This discrepancy is not understood. At low temperature, some datasets experience a drop of $\nu_{\rm eff}$ compatible with the mutual-friction dissipation model (see simulations and Oregon decay experiment) while the Prague experiments found no significant temperature dependence, in particular in the steady-state case. We have no explanation for this disagreement, but we note that it almost vanishes if the steady-state grid datapoint at 1.17 K is ignored, despite we found no sufficient reason to experimentally distrust it. Further pressure on this datapoint comes from the fact that as the temperature is lowered below 1 K, $\nu_{\rm eff}$ is known to drop further, as deduced from the Manchester turbulence decay experiments [30], which yielded $\nu_{\rm eff}/\kappa \approx 3 \times 10^{-3}$ in the $T \to 0$ limit.

Conclusions. – We have explored the concept of effective kinematic viscosity in steady-state turbulent He-II by experimental and numerical means, within $1.17\,\mathrm{K} \leq T \leq 2.16\,\mathrm{K}$. Our channel flow experiments revealed a robust scaling of vortex line density with mean flow velocity of the form $\mathcal{L} \propto V^{3/2}$, holding upon changing ρ_s/ρ_n by a factor 450. From this we inferred the validity of the heuristic definition of the effective viscosity, $\epsilon = \nu_{\rm eff}\,(\kappa\mathcal{L})^2$. The new values of $\nu_{\rm eff}$ deduced from our steady-state approach are consistent with known values deduced from decaying turbulence if we consider that an accurate determination of $\nu_{\rm eff}$ is in fact very difficult, both in decaying and steady-state turbulence, due to uncertainties in flow properties at large scales. This could be overcome in the future by exploring steady-state flows with well-known velocity statistics at large scales. Numerical simulations yield $\nu_{\rm eff}$ consistent with measurements in the range $1.35 \lesssim T \lesssim 2.05$ K. Outside this range the temperature dependence of simulations is steeper, requiring dedicated studies at these temperature extremes. The temperature dependence produced by the simulations can be usefully interpreted as a dissipative cross-over from a high temperature regime, where normal viscosity is the main dissipative process, to a low temperature regime where mutual friction becomes a significant one. This suggests that the temperature dependence $\nu_{\rm eff}(T)$ of turbulent He-II is an indicator of dissipation mechanisms. One contribution of this paper is to open the way for the determination of $\nu_{\rm eff}$ from a steady-state approach, making use and further validating governing equations already employed in analysis of QT decay.

* * *

We are grateful to the Ens de Lyon for providing access to PSMN computing center, supported by the Région Rhône-Alpes (CPER-CIRA) and EQUIP@MESO. E.V. and L.S. acknowledge grants GAČR 203/14/02005S and GAUK 366213, and P.-E.R. grant ANR-09-BLAN-0094.

REFERENCES

[1] Vinen W. F. and Niemela J. J., *J. Low Temp. Phys.* , **128** (2002) 167.
[2] Skrbek, L. and Sreenivasan, K. R., *Phys. Fluids 24*, **2012** (011301) .
[3] Nemirovskii S. K., *Physics Reports* , **524** (2013) 85.
[4] Fuzier S., Baudouy B. and Van Sciver S. W., *Cryogenics* , **41** (2001) 453.
[5] Salort J. *et al.*, *Phys. Fluids* , **22** (2010) 125102.
[6] Niemela J. J., Sreenivasan K. and Donnelly R. J., *J. Low Temp. Phys.* , **138** (2005) 537.
[7] Walmsley P. M. and Golov A. I., *Phys. Rev. Lett.* , **100** (2008) 245301.
[8] Chagovets T. V., Gordeev A. V. and Skrbek L., *Phys. Rev. E* , **76** (2007) 027301.
[9] Skrbek L. and Sreenivasan K. R., *Chapter 10 in Ten chapters of turbulence* (Cambridge University Press) 2013.
[10] Kondaurova L. and Nemirovskii S. K., *Phys. Rev. B* , **86** (2012) 134506.
[11] Smith M., Donnelly R. J., Goldenfeld N. and Vinen W. F., *Phys. Rev. Lett.* , **71** (1993) 2583.
[12] Stalp S., Skrbek L. and Donnelly R. J., *Phys. Rev. Lett.* , **82** (1999) 4831.
[13] Vinen W. F., *Phys. Rev. B* , **61** (2000) 1410.
[14] Skrbek L., Niemela J. J. and Donnelly R. J., *Phys. Rev. Lett.* , **85** (2000) 2973.
[15] Tennekes H. and Lumley J. L., *A first Course in Turbulence* (The MIT Press) 1994.
[16] Salort J., Roche P. E. and Leveque E., *Europhysics Lett. 94*, **2011** (24001) .
[17] Babuin S., Stammeier M., Varga E., Rotter M. and Skrbek L., *Phys. Rev. B* , **86** (2012) 134515.
[18] Roach P. E., *Int. J. Heat and Fluid Flow* , **8** (1987) 83.
[19] Lumley J. L. and McMahon J. F., *ASME J. Basic Eng.* , **89D** (1967) 764.
[20] Farell C. and Youssef S., *Journal of Fluids Engineering* , **118** (1996) 26.
[21] Comte-Bellot G. and Corrsin S., *Journal of Fluid Mechanics* , **25** (1966) 657.
[22] Salort J., Chabaud B., Leveque E. and Roche P. E., *Europhysics Lett. 97*, **2012** (34006) .
[23] Samuels D. C. and Kivotides D., *Phys. Rev. Lett.* , **83** (1999) 5306.
[24] Orszag S. and Patterson G., *Phys. Rev. Lett.* , **28** (1972) 76.
[25] Holmes D. S. and Van Sciver S. W., *J. Low Temp. Phys.* , **87** (1992) 73.
[26] Niemela J. J., Sreenivasan K. R. and Donnelly R. J., *J. Low Temp. Phys.* , **138** (2005) 534.
[27] Babuin S., Varga E. and Skrbek L., *J. Low Temp. Phys.* , (2013) .
[28] Wang R. T., Swanson C. E. and Donnelly R. J., *Phys. Rev. B* , **36** (1987) 5240.
[29] Swanson C. E., Wagner W. T., Donnelly R. J. and Barenghi C. F., *J. Low Temp. Phys.* , **66** (1987) 263.
[30] Golov A. I. and Walmsley P. M., *J. Low Temp. Phys.* , **156** (2009) 51.